Reference: *Biol. Bull.* **188:** 57–67. (February/March, 1995)

Elemental Distributions in Marine Bivalve Shells as Measured by Synchrotron X-Ray Fluorescence

KURT THORN[1,]*, ROBERT M. CERRATO[2], AND MARK L. RIVERS[1]

[1]*Department of Geophysical Sciences, University of Chicago, Chicago, Illinois 60637, and* [2]*Marine Sciences Research Center, State University of New York, Stony Brook, New York 11794-5000*

Abstract. The concentrations of elements from Mn to Pb in the shells of *Mercenaria mercenaria, Mya arenaria,* and *Argopecten irradians* were measured using synchrotron x-ray fluorescence. This technique provides sensitivity as low as 1 ppm and resolution of 8 μm. Elements were heterogeneously distributed, both on a large scale (several millimeters) and on a small scale (tens of micrometers). Large-scale variations were observed in the compositions of shell layers and in seasonal variations in strontium concentration. Small-scale changes in composition included elevated iron levels at the boundary between the prismatic and inner homogeneous shell of the hard clam, *Mercenaria mercenaria.* Variations in strontium concentrations were seen over time spans of several months, suggesting that this technique can be used to determine historical water temperatures. Elemental maps with a resolution of less than 10 μm were produced.

Introduction

The use of marine bivalves as environmental indicators has received considerable attention. Bivalves are believed to incorporate trace elements into their shells in proportion to the concentration of those elements in the water (Rhoads and Lutz, 1980). This incorporation is also influenced by other circumstances, including water temperature and salinity (Rosenberg, 1980). The incorporation of trace elements into marine bivalves could be used to monitor temporal changes in aspects of the marine environment, including the elemental composition and temperature of the water. Moreover, recent pollution could be studied, as well as paleoceanographic conditions. Strontium/calcium ratios have already been used as a method in paleothermometry that overcomes the limitations of the more common oxygen isotope paleothermometry (Beck *et al.,* 1992). Additionally, many bivalves produce visible growth increments in their shells, often as frequently as once per day. These growth increments provide a method of dating any observed changes in elemental composition of the shell.

When techniques like instrumental neutron activation analysis (INAA) and atomic absorption analysis are applied to whole shells of marine bivalves, heavy metal concentrations of less than 5 ppm by weight are reported (Al-Dabbas *et al.,* 1984; Koide *et al.,* 1982; Milliman, 1974). Carriker *et al.* (1982), using proton induced x-ray emission analysis (PIXE), reported concentrations of Cu and Zn in oysters (*Crassostrea virginica*) of 20 to 30 ppm weight. When such concentrations are measured by bulk analysis, fairly large amounts of shell are required for analysis, so resolution over short time scales is impossible.

All previous attempts to measure the distribution of elements within bivalve shells have been made with either PIXE microprobes or electron probe microanalysis (EPMA). Because the minimum elemental concentration measurable with EPMA is high, only those elements occurring in fairly high concentrations in the shell (Ca, Sr, Mg, S) can be observed (Wada and Suga, 1976; Rosenberg and Hughes, 1991). Three PIXE microprobe studies (Carriker *et al.,* 1982; Carell *et al.,* 1987; Swann *et al.,* 1991) report variations in heavy metal concentrations, but over fairly long (several month) time scales, although the excellent spatial resolution of the proton microprobe (3 μm) used by Carell *et al.* (1987) would have enabled

---

Received 29 October 1993; accepted 22 November 1994.

* Current Address: Whitespruce Dr., Wading River, NY 11792.

Abbreviations: SXRF, synchrotron x-ray fluorescence; PIXE, proton induced x-ray emission; EPMA, electron probe microanalysis; MDL; minimum detectable level.

them to study periods corresponding to 6–8 hours in young mussels.

In his analysis of bivalve shell chemistry, Rosenberg (1980) concludes that whole-shell analysis represents the elemental concentration incorrectly because elements are not necessarily distributed uniformly throughout the shell. Carriker *et al.* (1982) list several factors that influence the distribution of elements in shells, including structural and chemical changes that result from environmental fluctuations, fouling, adsorption, and weathering of the shell surface, elements adsorbed at shell surfaces and integrated into the shell matrix, and the heterogeneous distribution of elements within the shell.

The metal concentrations typically found in bivalve shells are considerably less than those measurable by EPMA and are near the 20 ppm detection limit of PIXE microprobes. Synchrotron x-ray fluorescence has minimum detection limits near 1 ppm, which should permit detection of these elements and resolution of variations in their concentration over short time scales.

This study attempts to evaluate the potential of synchrotron x-ray fluorescence as a technique for microanalysis of trace element distributions in bivalve shells of three species. Some samples were also analyzed with a PIXE microprobe in a pilot attempt to measure elemental distributions on scales down to 1 μm.

Materials and Methods

Preparation of shell sections

Three species were examined in this study: hard clams (*Mercenaria mercenaria*), soft-shell clams (*Mya arenaria*), and bay scallops (*Argopecten irradians*). Hard clams were obtained from a population in Moriches Bay, soft-shell clams from a population in Stony Brook Harbor, and scallops from a population in Peconic Bay. All collection locations were on Long Island, New York. Two types of sections were used in this study: thin sections (less than 250 μm thick) and thick sections (about 1 mm thick). For studies of *Mya arenaria,* sections were made of the chondrophore, an internal structure projecting from the hinge region. Sections of the chondrophore were used for analysis because the chondrophore contains better preserved growth lines than the main shell (Cerrato *et al.,* 1991). In addition, it is isolated from the environment, preventing damage and elemental contamination.

Shells were cleaned to remove adherent debris by scrubbing with a nylon brush in tap water. Thick sections were prepared by cutting a section from the shells along the axis of maximum growth. The cut surfaces were ground with successively finer silicon carbide grits and polished with aluminum oxide. The sections were then attached to cardboard mounts for synchrotron x-ray fluorescence analysis. Thin sections were prepared in the same manner as thick sections except that the shell sections, after grinding, were glued to pure SiO_2 glass slides with 5-minute epoxy. X-ray fluorescence analyses of the epoxy and slide indicated that they contained only trace amounts of zirconium and titanium. The mounted sections were resectioned to several hundred micrometers and ground to the desired thickness with successively finer silicon carbide grits. The sections were then hand polished with aluminum oxide. Previous x-ray fluorescence studies have shown that this process neither introduces significant amounts of elemental contamination nor smears the elemental distribution of the sample.

Shell microstructure

The shells of *Mercenaria mercenaria* are composed of three distinct shell layers: an outer prismatic layer and a middle and an inner homogeneous layer. The middle and inner homogeneous layers are separated by the pallial myostracum (Panella and MacClintock, 1968). All layers of the shell are aragonitic (Taylor *et al.,* 1973). During periods of stress, the organism ceases its growth and retracts its mantle, producing a translucent band, known as a growth break, in the shell. Daily growth lines are also visible in the shells of *Mercenaria mercenaria.* These consist of an aragonite-rich increment followed by a protein-rich line (Kennish, 1980).

Both the shell and the chondrophore of *Mya arenaria* contain daily growth patterns; however, the growth patterns in the chondrophore are much better preserved than those in the main shell. These growth increments are similar in form to those in *Mercenaria mercenaria*: they are composed of a thin line followed by a broad increment. It is not known whether they also exhibit the same pattern of protein-rich lines and calcium-carbonate-rich increments. The chondrophores also show strong seasonal patterns: they are opaque in spring, translucent in summer, and opaque in fall-winter. Winter and spring are separated by a prominent translucent spawning band (Cerrato *et al.,* 1991).

The shell of *Argopecten irradians* consists of an inner and an outer calcitic foliated layer separated by a middle aragonitic crossed-lamellar layer (Kennedy *et al.,* 1969). To our knowledge, these shells do not contain growth lines.

Synchrotron x-ray fluorescence analyses

Synchrotron x-ray fluorescence analyses were performed at beamline X26-A of the National Synchrotron Light Source at Brookhaven National Laboratory. Samples were mounted in a sample holder in air. X rays produced by the synchrotron travel 9 m through an evacuated pipe to the sample. The x rays produced by the synchrotron have a critical energy of 5 keV and travel through several beryllium windows (total Be thickness = 1 mm) and 35 mm of air before striking the sample. The air path of the fluorescent x rays sets the effective lower detection limit at argon (Z = 18). The x-ray beam is collimated by an 8 μm tantalum pinhole immediately before striking the sample. This produces a microbeam, allowing resolution of fine structures. Immediately upstream of the collimator, the intensity of the x-ray beam is measured by an ion chamber.

The samples were mounted on an X, Y, Z, θ stage. They could thus be rastered under the x-ray beam, allowing the measurement of elemental concentrations at different points as well as along one- and two-dimensional scans over the specimen. An optical microscope imaging the specimen permitted precise determination of the location being analyzed. The secondary x rays emitted by the sample are collected in a Si(Li) detector. The detector was filtered with 500 μm of Kapton film, to reduce the count rate from the Ca x rays. This prevents saturation of the detector. The spectra are then stored in a Micro Vax computer for further analysis. Minimum detectable levels (MDLs) were 5 ppm for Mn, 2.5 ppm for Fe and Pb, 2 ppm for Sr, and 1.5 ppm for Ni through Br, for a spectrum collected for 4 min. MDLs were calculated by measuring the background under these peaks in a typical x-ray spectrum and computing the elemental concentration of a peak with an area equal to three standard deviations of the background. The calculated concentrations from the spectra were used to standardize these measurements.

The sample is mounted with the surface oriented at 45 degrees to the incoming x-ray beam and the detector. This exploits the angular distribution of the scattered radiation to minimize background. However, it also results in the beam traveling relative to the face of the sample as it penetrates the sample. This prevents the detection of changes in elemental concentration over small areas perpendicular to the beam. This effect is more pronounced at higher x-ray energies. At Ca (3.69 keV) the horizontal travel is only 11 μm; at Sr (14.14 keV) it is 55 μm. To reduce this effect, one can make thinner samples; however, it becomes difficult to optically resolve growth lines in samples thinner than 100 μm. Thus, the samples were oriented so that the interfaces of interest were parallel to the incoming beam whenever possible.

Spectra can be recorded in one of two ways: either the entire spectrum collected by the detector is recorded, or the net areas of the peaks of interest are recorded. Generally, when analyzing individual points, the entire spectrum was saved, as this allowed a more sophisticated background and peak-fitting routine to be used. However, when scanning a region, generally only the net areas of the peaks were saved, because this greatly reduces data analysis time. The Micro Vax implements automated scanning routines that allow the collection of data over long scans with no user intervention. The setup of the x-ray microprobe is discussed more comprehensively by Gordon *et al.* (1990).

Absolute concentrations were determined from the peak areas fit to the spectra by use of a "standardless" analysis program (NRLXRF). Using fundamental parameters, this program predicts the relative intensities for the different x-ray lines in the spectrum. These predictions are based on the thickness of the sample, the filtering conditions, and the assumed concentrations. The concentration of Ca was assumed to be 40% by weight, and was used as an internal standard to calculate the composition by comparing the predicted intensities and the actual count intensities. It was checked by predicting known standards that were measured at the beginning of each measurement session. The error was typically less than 5%.

PIXE microprobe analyses

Several samples were also analyzed by proton induced x-ray emission (PIXE) at the University of Melbourne. Analyses were performed with a 3 MeV proton beam, magnetically focused to 1 and 4 μm. Samples were thick shell sections, mounted in vacuum. The secondary x rays were collected with a Si(Li) detector, which was generally filtered with 50 μm Al to reduce the Ca count rate. However, some analyses were performed without filters in an attempt to measure sulfur concentrations. Rutherford backscattering spectroscopy (RBS) analyses were also made to allow carbon and oxygen concentrations to be measured.

PIXE analyses were made by sweeping the beam over a predetermined region of interest in the shape of an unclosed lissajous figure. Every time an x-ray event is detected by the Si(Li) detector, the energy of the event and the x and y coordinates of the beam are recorded. The x-ray spectrum is generated by disregarding the x and y values and simply taking the energy spectrum. A map of the concentration of a given element can then be generated by placing a window over a given peak and plotting the intensity of events in that energy range as a function of x and y. Analyses were performed on scales from 30 by 30 μm to 100 by 100 μm and were generally collected for 30 min. The MDLs in calcium carbonate matrix were about 18 ppm for Zn and Fe. This microprobe is described in more detail in Legge *et al.* (1986).

Although the PIXE microprobe does not have elemental sensitivity as good as the synchrotron x-ray fluorescence microprobe, it does have substantially better position resolution (a beam spot of 1 μm rather than 8 μm). The mean x-ray production depth for proton excitation in calcium carbonate is also less than that of x-ray excitation. Both of these factors enabled higher resolution of trace element distributions in the shell, but increased the MDLs for many elements.

Results

Surface contamination

Both shell surfaces of all species studied were found to be extremely contaminated with many trace elements. Table I lists the concentrations of these elements on both the exterior and interior surfaces of several organisms. Transverse scans across sections of scallop and hard clam shells showed that metal concentrations were much higher on both the interior and exterior surfaces of the shell than they were within the main shell. A representative transect is shown in Figure 1. Most elements were more concentrated on the exterior surface than the interior surface. However, the ratio of surface to main shell concentrations varied widely from element to element. The Ni concentration was only 1.5 times greater on the exterior surface, but the Cu concentration was 4.5 times greater. This is not unexpected, as the processes by which the elements are deposited on these surfaces are very complex. Scans in hard clams showed similar results. Trace element contamination on the interior shell surface is present in only a very thin layer. Within 100 μm the trace element contamination drops by a factor of 20–50, typically to within a factor of 2 of its average concentration. Most elements on the exterior surface of the hard clam behave in the same way as those on the interior surface, except iron (Fig. 2). Iron concentrations peaked both near the surface (30 μm) and farther in (180 μm). This is probably due to the periostracum and adherent debris on the shell surface; but why only Fe is affected is not known. The other trace elements are present in a surface layer that contains little calcium. This effect was most pronounced on the external surface; the maximum trace metal concentrations were at 30 μm from the edge of the shell and about 240 μm from where calcium concentrations became constant.

Shell layers

Most trace and minor elements (including Sr) are preferentially incorporated into the prismatic shell of the hard clam. The ratio of concentration in the prismatic shell to concentration in the homogeneous shell varied considerably from element to element, from about 20 for Fe to 1.5 for Sr. The reason for this increased concentration is unknown. Similar differences between shell layers were observed in scallops. Sr concentration in scallops was inversely related to both Mn and Fe concentrations; and Sr concentrations were highest in the outer 500 μm of shell, while Mn concentrations were highest in the inner 400 μm of shell. Some feature of the biological precipitation process is influencing the trace element concentration, as the

Table I

Elemental concentrations (ppm) in selected marine bivalves

Location	Mn	Fe	Ni	Cu	Zn	Br	Sr	Pb
Scallops (*Argopecten irradians*)								
Exterior surface	262	1080	152	902	308	17	814	21
Interior surface	208	636	102	201	106	21	1300	21
Outer shell layer	34 ± 1.4	8.5 ± 3.5	2 ± 0	2.5 ± 2.1	3 ± 1.4	1 ± 0	1495 ± 106	2 ± 0
Inner shell layer	48.5 ± 5	8.5 ± 3.5	2 ± 0	2 ± 0	5 ± 1.4	2 ± 1.4	911.5 ± 18	5 ± 2.1
Hard-shell clams (*Mercenaria mercenaria*)								
Prismatic shell	12.4 ± 3	219 ± 59	<1.5	3.6 ± 2.2	<1.5	5.4 ± 0.8	1247 ± 448	<2.5
Prismatic (DEC)	8.3 ± 3.9	38.8 ± 35	2.8 ± 1.5	1.5 ± 0.6	1.5 ± 0.6	3 ± 0	1139 ± 211	1 ± 0
Prismatic (PIXE)	9.8 ± 15	349 ± 518	<18	<18	13 ± 6.8	12.8 ± 8.3	3832 ± 961	
Prism./homog. boundary	3.5 ± 2.1	1085 ± 302	<1.5	3.3 ± 0.4	<1.5	5.5 ± 1.1	1115 ± 345	<2.5
Middle homog. shell	7.2 ± 2.2	11.6 ± 7.3	<1.5	3 ± 0.9	<1.5	5.4 ± 0.5	984 ± 353	<2.5
Middle homog. (DEC)	6.8 ± 8.2	4 ± 4.1	1 ± 0.8	1.8 ± 0.5	1.3 ± 0.5	2 ± 0	1007 ± 336	2.3 ± 2.5
Middle homog. (Thick)	1.25 ± 0.5	<2.5	1 ± 0	1 ± 0	1.5 ± 0.6	2.5 ± 1.3	725 ± 132	1 ± 0
Inner homog. (DEC)	1.8 ± 1.3	2.8 ± 2.5	1 ± 0	3 ± 2.6	1.4 ± 0.6	1.4 ± 0.6	1673 ± 180	1.7 ± 0.6
Soft-shell clams (*Mya arenaria*)								
Chondrophore	10 ± 4.4	<2.5	<1.5	<1.5	2 ± 0.6	<1.5	1383 ± 133	<2.5

All concentrations are in parts per million. Errors are given as the standard deviation of multiple measurements within the same shell layer; they do not reflect measurement error. Numbers without listed errors are based on single measurements. DEC: Shells came from collections in waters closed by the Department of Environmental Conservation. Thick: Data were taken on shell thick sections.

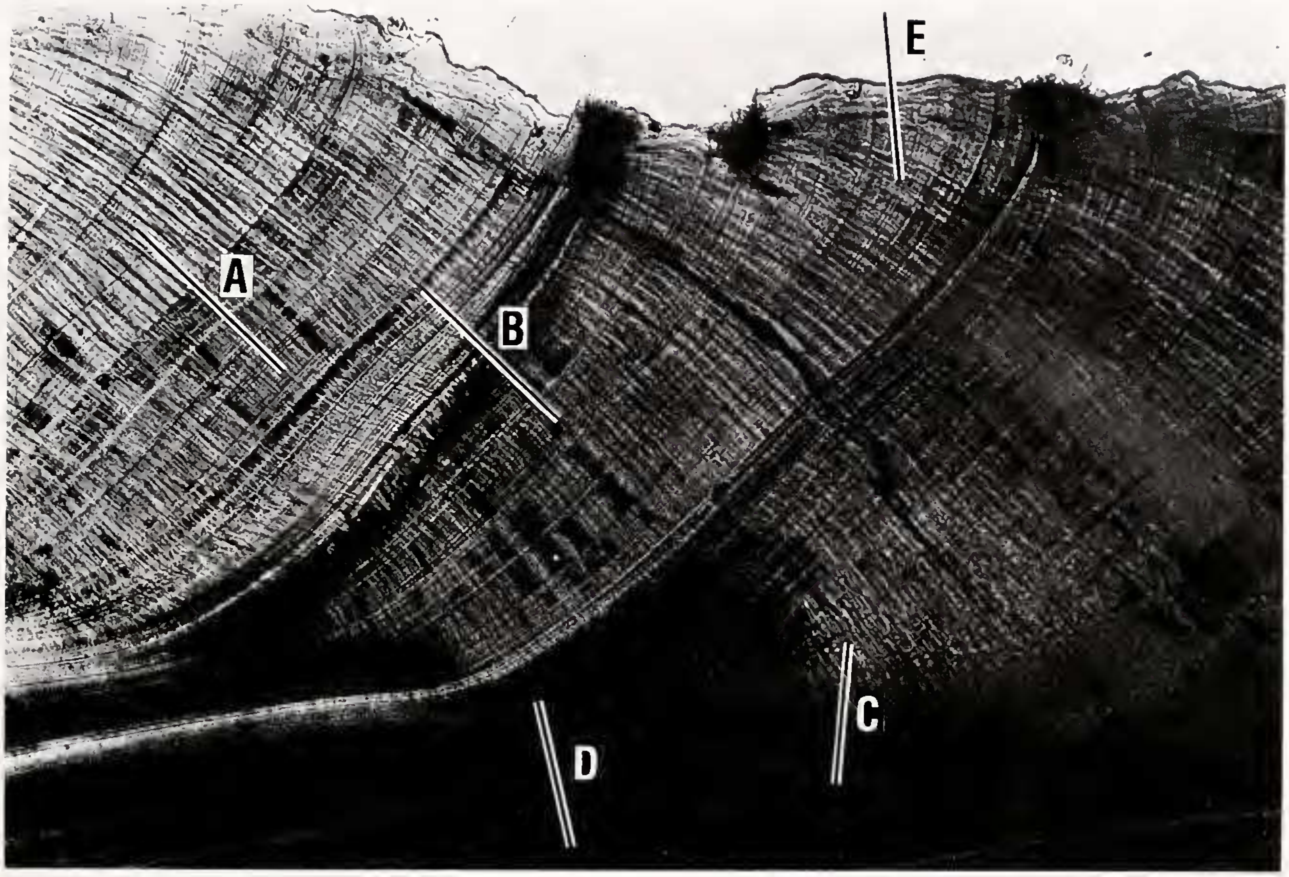

Figure 1. Representative transects along which scans were taken in *Mercenaria mercenaria* (A) Transect across daily growth increments in prismatic shell. (B) Transect across growth break. (C) Transect across prismatic-homogeneous boundary. (D) Transect across daily growth increments in homogeneous shell. (E) Transect across exterior shell surface.

chemistry of the scallop shell does not behave like geological carbonates. However, differences in chemical composition between biologically precipitated carbonates and geologically precipitated carbonates are not unknown; Buchardt and Fritz (1978) described aragonitic shell precipitated by a freshwater gastropod in which the strontium concentration of the shell is 5 times less than that of geologically precipitated aragonite under the same conditions. In addition, White *et al.* (1977) showed that Mn can replace Ca in aragonite formed by *Mya arenaria,* whereas this is not possible in geologically precipitated aragonite.

At the boundary between the prismatic shell and the middle homogeneous shell in the hard clam, very pronounced changes in elemental composition were observed (Figs. 3, 1). At this boundary, iron concentrations are typically 4.5 times greater than in the prismatic shell and 100 times greater than in the homogeneous shell. This iron peak is very narrow, about 40 μm wide, and was present in every measurement made across this boundary. The peak was always within 50 μm of where the boundary was located optically. Strontium concentrations declined between the prismatic and the homogeneous boundary, but this occurred more gradually, over about 100 μm, and appears to be associated only with the difference in Sr concentration in the two shell layers. Sr concentration reaches its nominal concentration in homogeneous shell at the same location as the peak in iron concentration. Manganese concentrations are lower at this boundary than in either the prismatic shell or the homogeneous shell, perhaps because the much greater concentration of iron is occupying the sites in the crystal lattice that are normally occupied by manganese. No feature similar to this has been observed in other organisms to our knowledge.

Sr concentration maps

Both the x-ray microprobe and the proton microprobe can be used to make high-resolution elemental maps, so changes in elemental concentration can be explored over very small areas. And with bivalve shells, fine variations

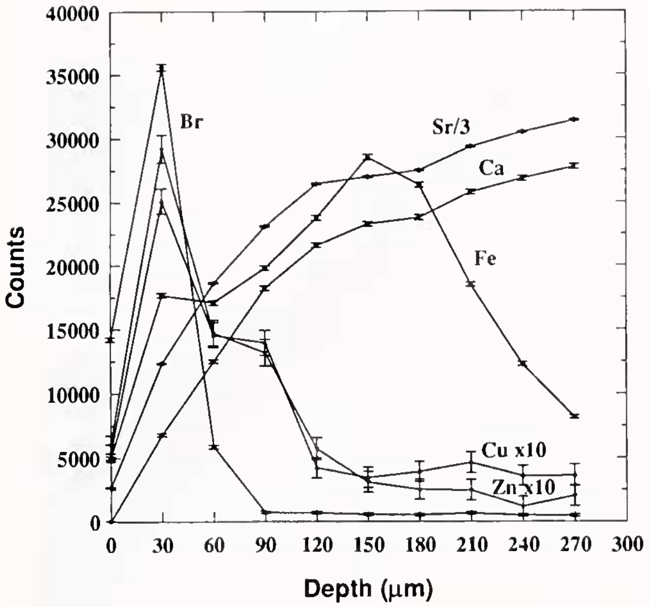

Figure 2. Scan across the outer surface of a *Mercenaria mercenaria* thick section. Data were recorded as individual spectra at each point. The spectra were then fitted to a sum of gaussian peaks and a background. The counts reported are the net areas of the peaks, less the background. Data was recorded for 40 s per point (detector live time).

with ontogeny can also be studied. We have used this scanning ability to elucidate changes within the shell structure, as with the prismatic-homogeneous boundary described above; but we have also measured the variations of trace element concentrations with time. The measurements of strontium were most successful. Because of its high concentration in the shell, strontium can be measured very accurately with counting times of only 5 s at each point in the shell. One-dimensional scans can therefore be made very quickly: a millimeter can be scanned at 10-μm resolution in less than 10 min. We could easily map a 2-year area of shell deposition at a resolution of a few days (Fig. 4) and produce very high-resolution two-dimensional elemental maps. A map of the hinge region of *M. mercenaria* is shown in Figure 5. Note the very good correlation between the strontium concentration and the banding in the thin section. Such scans are also possible for other elements, though reduced concentrations require proportionally longer counting times. Scans to measure Fe concentration were typically recorded at 30 s per point. For elements at levels of a few parts per million, counting times of several minutes are necessary.

High-resolution maps of Sr concentration made with the PIXE microprobe have shown variations in Sr concentration over scales as small as 10 μm. These variations appear to be correlated with the presence of growth breaks. However, because only a few PIXE measurements were made, this is not conclusive.

Growth lines

A comprehensive attempt was made to find trace element correlations with the daily microgrowth lines in the prismatic shell of *M. mercenaria*. The results strongly suggest that, although there is variation in trace element concentration in the prismatic shell of *M. mercenaria*, it is not necessarily correlated with the presence of microgrowth lines. All scans showed that iron concentration in the prismatic shell was nonuniform, but in most cases, no correlation with the microgrowth lines could be made. However, one scan (nsls106.10) showed very high correlation between the microgrowth lines and fluctuations in the iron content. In that scan, every microgrowth line was accompanied by a drop in iron concentration. Other scans showed some correlation between the presence of microgrowth lines and iron concentration, but none was as pronounced as this one. In an effort to improve the detectability of any iron fluctuations, we oriented samples so that the microgrowth lines were parallel to the incident beam. Thus, as the beam penetrated, it would stay within the microgrowth lines rather than transversing them. In addition, images were captured digitally after the beam position had been determined, enabling precise comparison between the image and the elemental concentration. Neither of these improvements showed further correlations between iron concentration and the presence of microgrowth lines. PIXE microprobe analyses were not sensitive enough to detect variations in the iron concentration of less than 40 ppm, and no structures were seen in the PIXE measurements of iron concentration. A correlation between microgrowth lines and iron concentration in the shell seems unlikely, but this is an area deserving further study.

Discussion

Synchrotron x-ray fluorescence (SXRF) microprobes provide lower minimum detectable levels than PIXE and EPMA microprobes. The experimentally determined MDL for Fe in thick clamshell sections was 3 ppm for SXRF and 18 ppm for PIXE. Our experience is that PIXE microprobes can make much larger and higher resolution maps than SXRF microprobes, although at lower sensitivity. PIXE measurements are generally made for long times (30 min) over large areas (1000 μm^2), whereas SXRF measurements are made for short times (1 min) over small areas (64 μm^2). Electron microprobes have MDLs of several hundred parts per million, worse than either PIXE or SXRF. But electron microprobes are typically more sensitive to low-Z elements than SXRF and PIXE microprobes (Janssens *et al.*, 1992). The minimum spot size of the NSLS microprobe is 8 μm; for EPMA and PIXE mi-

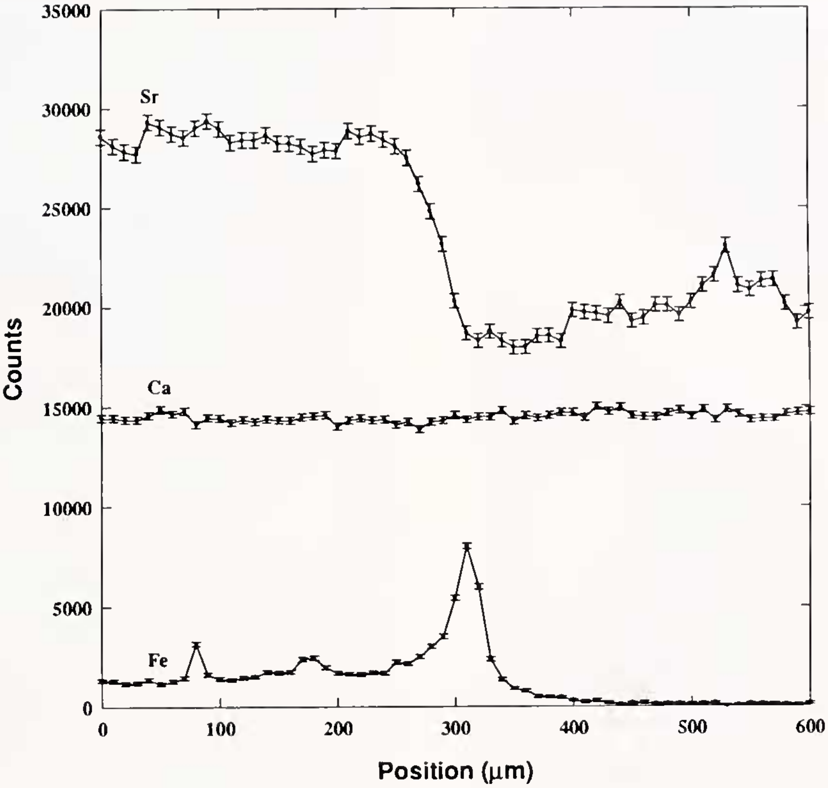

Figure 3. Scan across the prismatic/homogeneous boundary in a *Mercenaria mercenaria* thin section. Data were recorded as the area under user-defined regions of interest, with the background subtracted. Data was recorded for 15 s per point (detector live time). Initial Fe concentration is 211 ppm, initial Sr concentration is 1550 ppm. The Fe peak concentration is 1420 ppm.

croprobes it is 1 μm. New PIXE microprobes claim spot sizes of 300 nm.

For low-Z elements ($Z < 18$) EPMA has the greatest sensitivity as well as small spot size. Because of the ready availability of electron microprobes, EPMA is also suited to measurements of higher-Z elements present in quantities of several hundred parts per million or more. For measurements of elements present in concentrations of a few parts per million, SXRF is the method of choice. This is the only technique that combines MDLs of a few parts per million with spot sizes of a few micrometers. However, for some measurements, the spot size of the NSLS microprobe (8 μm) is too large. In these cases, PIXE microprobes can be used, if the elements are present in large enough concentrations. The greater accessibility of PIXE microprobes also makes them attractive for studies of elements present in concentrations of several tens of parts per million.

Bulk analysis techniques cannot provide the same spatial resolution as microprobes. The neutron activation studies of Carell *et al.* (1987) were performed on shell samples of 10–50 mg. This corresponds to a shell section 0.5 mm thick by 6 mm long by 3 mm deep. If this section is cut with the thin direction normal to the ventral margin, it represents approximately 1 month of growth. Atomic absorption analysis can detect much smaller amounts of trace elements, hence the limiting factor is the size of the shell section that can be obtained. This probably limits bulk analysis techniques to time resolutions of a few weeks. In addition, many clamshell sections must be prepared to make a study at this resolution over a significant period. In contrast, microprobe techniques require only one section per shell. Consequently, bulk analysis techniques are suitable for situations where resolution of small time scales is not necessary and integration of elemental concentrations over all dimensions of the shell is not a problem. In practice, microprobe techniques are probably more suitable for time-resolved studies of trace elements in bivalve shells. Bulk analysis methods can, however, detect elemental concentrations a factor of a thousand smaller than microprobes can.

Wavelength-dispersive detectors should improve the usefulness of SXRF microprobes for analyzing trace elements in bivalve shells. Because wavelength-dispersive

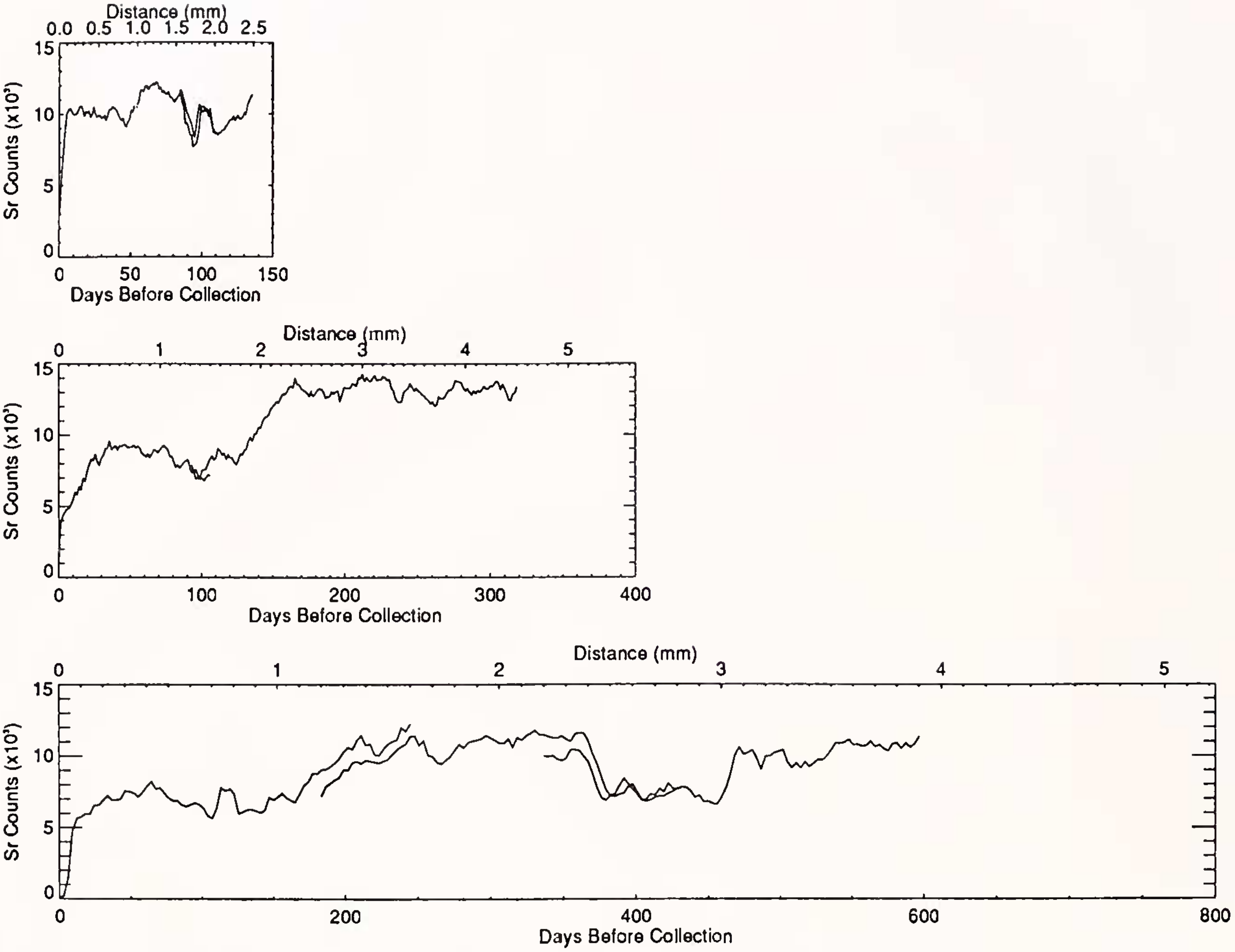

Figure 4. Variation in Sr concentration across growth increments in the chondrophore of *Mya arenaria*. Each of the three scans was taken on a different shell; all shells were harvested at the same time. Distance is measured in millimeters from the ventral margin of the chondrophore. Time before harvesting was calculated by dividing the distance from the margin by the average growth rate per day, which was determined by measuring the distance from the margin to the spawning break which occurred approximately 90 days before harvest. Each plot consists of three separate scans separated by up to 150 μm parallel to the growth increments. Notice the strong correlation of variations in each of the separate scans. Note also the correlations between the shells. We believe that these variations represent changes in the water temperature over time.

spectrometers detect only a single x-ray wavelength, they eliminate the filtering necessary to prevent saturation of an energy-dispersive detector by Ca x rays. This filtering also attenuates other low-energy x rays, preventing the detection of low-Z elements and resulting in high (200 ppm) MDLs for Ti. Use of a wavelength-dispersive detector would allow the detection of much smaller quantities of low-Z elements, and possibly improve MDLs for higher-Z elements as well. Such a device is now in use at the National Synchrotron Light Source at Brookhaven National Laboratory (Rivers *et al.*, 1992). Future SXRF microprobes will become even more useful as they are developed at third-generation synchrotrons, such as the Advanced Photon Source (APS) at Argonne National Laboratory. A planned SXRF microprobe at the APS will have 10^4 times more photons in a given energy range. This will allow the use of extremely small spot sizes (0.1 μm) at current detection limits, or lower detection limits at small spot sizes (1 μm).

SXRF microprobes are not limited merely to the applications discussed here. It is also possible to use SXRF to study other calcified samples, such as corals or fish otoliths. Studies of fish otoliths with EPMA (Gunn *et al.*, 1992) and PIXE (Gauldie *et al.*, 1992) suggest that the

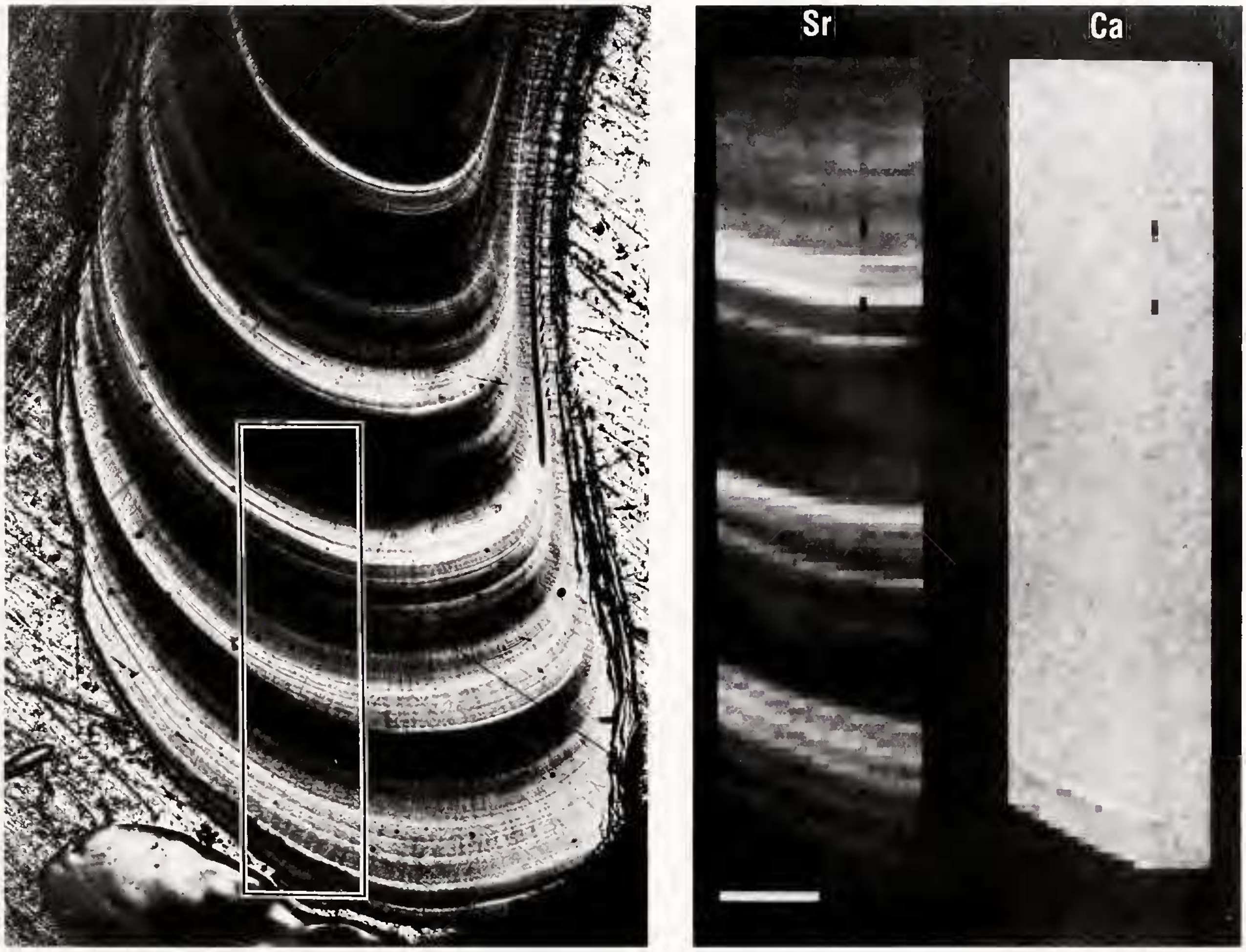

Figure 5. Two-dimensional scan (map) of Sr and Ca concentration in the hinge region of *Mercenaria mercenaria.* Each pixel measures 20 μm on a side, and was collected for 20 s. The data were recorded as background-subtracted regions of interest and have been normalized to beam intensity and detector live time. The box on the photomicrograph approximately corresponds to the region scanned. Note the correlation of the variations in strontium concentration with the seasonal banding in the chondrophore.

SXRF microprobe would be a valuable tool for such studies. Spatial resolution and elemental sensitivity similar to that obtained here should be achievable in studies of other calcified samples. Furthermore, it is not necessary to sacrifice the molluscs and section their shells to use the SXRF microprobe. Because the beam deposits relatively little energy in the shell and stops within the first few hundred micrometers of the shell, live molluscs can be studied, though this raises the problems of removing surface contamination and dating the sampled positions accurately. SXRF can also be used to detect organometallic compounds, provided the metals are of sufficiently high Z. Techniques such as extended x-ray absorption fine structure (EXAFS) also promise the ability to determine the oxidation state of metals detected by SXRF.

The measurements made on bivalve shells have revealed several interesting features. The contamination of the exterior surface is most likely due to the adsorption of elements onto the calcium carbonate from seawater. However, the contamination could also be due to adherent debris on the surface of the shell. The contamination of the interior surface is probably not due to elements adsorbed onto the calcium carbonate during active growth, because they would then have to be removed before additional shell was deposited. Although there is some evidence that the shell undergoes structural changes after deposition (Gordon and Carriker, 1978), it seems more likely that the elemental contamination arose after the shells were collected, either from adsorption of metals from the pallial fluid or from contamination after collection.

Seasonal variations in strontium concentration were observed in the shells of both hard- and soft-shell clams (Fig. 4). Differences in strontium concentration of 30% to 40% were typical between winter and summer. Each of the high and low Sr regions was about 180 days long. We believe these variations are a result of the seasonal temperature change of the seawater. In addition, shorter-term variations (100 μm long) were observed; these probably correspond to shorter-term temperature variations. As with paleothermometry done with Sr/Ca ratios in corals (Beck *et al.*, 1992), our results show that increases in Sr concentration correspond to decreases in temperature. Assuming that the change in Sr concentration is linearly related to the change in water temperature, the change in the observed Sr count rate is 18 counts/s/C°. In a 10-s per point scan, changes of 6 counts/s are observable. This corresponds to a temperature change of 0.33°C. The use of x-ray fluorescence to measure small (0.3°C) temperature variations over short (3-day) time scales seems quite simple. In practice, the resolution is probably limited by the rate at which shell strontium concentrations equilibrate to the ambient water temperature. Our scans show good correlation between different transects on an individual shell and between different shells harvested from the same location at the same time. This strongly suggests that we are observing environmental effects upon the shell. Figure 5 also shows very good correlation between Sr concentration and seasonal banding in the shell.

One problem complicating the use of x-ray fluorescence as a means of paleothermometry using Sr/Ca ratios is that for samples thinner than 200 μm, sample thickness influences the Sr count rate. This is especially a problem near the edges of shells, which were often inadvertently ground thinner during preparation than other parts of the shell. Such "thickness effects" show up as a gradual increase in the Sr (and in extreme cases Ca) count rate as the sample is scanned. In practice, the best way to avoid such effects is to use samples thicker than the mean fluorescence depth for Sr K x rays, because preparing samples uniform in thickness to within a few percent is difficult to do. In that case, the Sr count rate is unaffected by small variations in sample thickness.

The synchrotron x-ray fluorescence microprobe has significant advantages for trace element analyses in calcified structures. It combines very low detection limits with very small spot sizes. This allows the measurement of elemental concentrations as low as 1 ppm over scales as small as 10 μm. Synchrotron x-ray fluorescence microprobes have significantly better detection limits than EPMA and PIXE microprobes, and are probably the best instrument for most studies of trace element distributions in calcified structures. When structures smaller than 10 μm are to be resolved, the extremely small spot size of PIXE microprobes makes them the analytical technique of choice.

Acknowledgments

We are grateful to David Jamieson for performing the PIXE and RBS analyses at the University of Melbourne.

Literature Cited

Al-Dabbas, M. A. M., F. H. Hubbard, and J. McManus. 1984. The shell of *Mytilus* as an indicator of zonal variations of water quality within an estuary. *Estuarine Coastal Shelf Sci.* **18:** 263–270.

Beck, J. W., L. R. Edwards, E. Ito, F. W. Taylor, J. Recy, F. Rougerie, P. Joannot, and C. Henin. 1992. Sea-surface temperature from coral skeletal strontium/calcium ratios. *Science* **257:** 644–647.

Buchardt, B., and P. Fritz. 1978. Strontium uptake in shell aragonite of the freshwater gastropod *Limnaea stagnalis. Science* **199:** 291–292.

Carell, B., S. Forberg, E. Grundelius, L. Henrikson, A. Johnels, U. Lindh, H. Mutvei, M. Olsson, K. Svaerdstroem, and T. Westermark. 1987. Can mussel shells reveal environmental history? *Ambio* **16:** 2–10.

Carriker, M. R., C. P. Swann, and J. W. Ewart. 1982. An exploratory study with the proton microprobe of the ontogenetic distribution of 16 elements in the shell of living oysters. *Mar. Biol.* **69:** 235–246.

Cerrato, R. M., H. V. E. Wallace, and K. G. Lightfoot. 1991. Tidal and seasonal patterns in the chondrophore of the soft-shell clam *Mya arenaria. Biol. Bull.* **181:** 307–311.

Gauldie, R. W., G. C. Coote, K. P. Mulligan, and I. F. West. 1992. A chemical probe of the microstructural organization of fish otoliths. *Comp. Biochem. Physiol.* **102A:** 533–545.

Gunn, J. S., I. R. Harrowfield, C. H. Proctor, and R. E. Thresher. 1992. Electron probe microanalysis of fish otoliths—evaluation of techniques for studying age and stock discrimination. *J. Exp. Mar. Biol. Ecol.* **158:** 1–36.

Gordon, J., and M. R. Carriker. 1978. Growth lines in a bivalve mollusk: subdaily patterns and dissolution of the shell. *Science* **202:** 519–521.

Gordon, B., A. L. Hanson, K. W. Jones, J. G. Pounds, M. L. Rivers, G. Schidlovsky, P. Spanne, and S. R. Sutton. 1990. The application of synchrotron radiation to microprobe trace element analysis of biological samples. *Nucl. Inst. Meth.* **B45:** 527–531.

Janssens, K. H., F. van Langevelde, F. C. Adams, R. D. Vis, S. R. Sutton, M. L. Rivers, K. W. Jones, and D. K. Bowen. 1992. Comparison of synchrotron X-ray microanalysis with electron and proton microscopy for individual particle analysis. *Adv. X-Ray Anal.* **35B:** 1265–1275.

Kennedy, W. J., J. D. Taylor, and A. Hall. 1969. Environmental and biological controls on bivalve shell mineralogy. *Biol. Rev.* **44:** 499–530.

Kennish, M. J. 1980. Shell microgrowth analysis: *Mercenaria mercenaria* as a type example for research in population dynamics. Pp. 255–294 in *Skeletal Growth of Aquatic Organisms.* D. C. Rhoads and R. A. Lutz, eds. Plenum, New York.

Koide, M., D. S. Lee, and E. D. Goldberg. 1982. Metal and transuranic records in mussel shells, byssal threads and tissues. *Estuarine Coastal Shelf Sci.* **15:** 679–695.

Legge, G. J. F., C. D. MacKenzie, A. P. Mazzolini, R. M. Sealock, D. N. Jamieson, P. M. O'Brien, J. C. McCallum, G. L. Allan, R. A. Brown, R. A. Colman, B. J. Kirby, M. A. Lucas, J. Zhu, and J. Cerini. 1986. Microbeam imaging at micron and submicron resolution. *Nucl. Inst. Meth.* **B15:** 669–674.

Milliman, J. D. 1974. Marine Carbonates, Part I of *Recent Sedimentary Carbonates.* Springer-Verlag, New York. 375 pp.

Panella, G., and C. MacClintock. 1968. Biological and environmental rhythms reflected in molluscan shell growth. *J Paleontol.* **42:** 64–80.

Rivers, M. L., K. Thorn, S. R. Sutton, and K. W. Jones. 1992. Wavelength dispersive detectors in synchrotron x-ray fluorescence microprobe analysis. *EOS, Trans. Am. Geophys. Union.* 73(43): 620.

Rhoads, D. C., and R. A. Lutz. 1980. Skeletal records of environmental change. Pp. 1–19 in *Skeletal Growth of Aquatic Organisms.* D. C. Rhoads and R. A. Lutz, eds. Plenum, New York.

Rosenberg, G. D. 1980. An ontogenetic approach to the environmental significance of bivalve shell chemistry. Pp. 133–168 in *Skeletal Growth of Aquatic Organisms.* D. C. Rhoads and R. A. Lutz, eds. Plenum, New York.

Rosenberg, G. D., and W. W. Hughes. 1991. A metabolic model for the determination of shell composition in the bivalve mollusc, *Mytilus edulis. Lethaia* **24:** 83–96.

Swann, C. P., K. M. Hansen, K. Price, and R. Lutz. 1991. Application of PIXE in the study of shellfish. *Nucl. Inst. Meth.* **B56/57:** 683–686.

Wada, K., and S. Suga. 1976. The distribution of some elements in the shell of freshwater and marine bivalves by electron microprobe analysis. *Bull. Natl. Pearl Res. Lab* **20:** 2219–2240.

White, L. K., A. Szabo, P. Carkner, and N. D. Chasteen. 1977. An electron paramagnetic resonance study of manganese(II) in the aragonite lattice of a clam shell, *Mya arenaria. J. Phys. Chem.* **81(14):** 1420–1424.